Molecular Vision 2018; 24:746-758 <http://www.molvis.org/molvis/v24/746>
Received 31 March 2018 | Accepted 23 November 2018 | Published 25 November 2018

Echinacoside protects retinal ganglion cells from ischemia/reperfusion-induced injury in the rat retina

Lin Li,[1] YeFei Wang,[1] XiuHong Qin,[2] Jing Zhang,[1] ZhenZhen Zhang[1]

(The first three authors contributed equally to this paper.)

[1]Department of Ophthalmology, Shanghai Ninth People's Hospital, Shanghai Jiao Tong University School of Medicine, Shanghai, China; [2]Department of Ophthalmology, First Affiliated Hospital of Dalian Medical University, DaLian, Liaoning Province, China

Objective: To investigate whether echinacoside (ECH) protects the retina against ischemia/reperfusion (I/R) injury and the underlying mechanisms.

Methods: Adult male Wistar rats were randomly divided into four groups: sham, sham plus ECH, I/R plus vehicle, and I/R plus ECH. Before the retinal I/R injury produced by high intraocular pressure (HOP), ECH was administered (20 mg/kg daily) for 7 days. The level of retinal cell damage was evaluated using Fluoro-Gold (FG) retrograde labeling and terminal deoxynucleotidyl transferase-mediated dUTP nick end-labeling (TUNEL) analysis 7 days after I/R. Optic nerve histology was analyzed with transmission electron microscopy. Levels of retinal malondialdehyde (MDA), superoxide dismutase (SOD), catalase (CAT), and glutathione peroxidase (GSH-Px) were determined. The expression of apoptosis-associated factors (Apaf-1, Parp, and Bad) were analyzed with western blotting and quantitative real-time PCR (qPCR). The production of proinflammatory cytokines (tumor necrosis factor-α [TNFα], interleukin-1 beta [IL-1β], and IL-6) was analyzed with enzyme-linked immunosorbent assay (ELISA) 7 days after the I/R injury as well.

Results: The administration of ECH not only preserved retinal morphology but also attenuated retinal inflammation and apoptosis at 7 days after the I/R injury and decreased I/R-induced oxidative stress in the retina statistically significantly.

Conclusions: ECH protected against I/R-induced retinal injury, via activation of antioxidant enzymes and suppression of inflammation. Therefore, ECH could be a potential therapeutic candidate for the treatment and management of I/R retinal diseases.

Ischemia/reperfusion (I/R) injury is a common etiology in many retinal diseases, including retinal vascular occlusion, acute glaucoma, retinopathy of prematurity, age-related macular degeneration, and diabetic retinopathy [1,2], and leads to a loss of vision. As the retina is highly dependent on its oxygen supply and very sensitive to an impaired blood flow, I/R-induced oxidative stress is thought to be the direct cause of retinal injury [3].

Furthermore, I/R injury is known to increase the levels of reactive oxygen species (ROS) that can lead to apoptosis and necrosis [4], which are important regulators of cell death. ROS are a variety of molecules and free radicals derived from molecular oxygen that is reintroduced during reperfusion, including hydroxyl radical, superoxide, singlet oxygen, and hydrogen peroxide (H_2O_2) [5]. Free radicals induce the destruction of polypeptide chains and amino acids, and fragmentation of DNA molecules, the latter of which leads to activation of poly(ADP-ribose) polymerase (PARP) to produce poly(ADP-ribose; PAR). Then PARP cleaves nicotinamide adenine dinucleotide (NAD), resulting in energy failure and cell death [6]. Our previous studies have shown that retinal malondialdehyde (MDA) levels and superoxide dismutase (SOD), catalase (CAT), and glutathione peroxidase (GSH-Px) activity are indicators of oxidative stress and reflect the severity of the retinal injury [7].

Inflammation is a pathologic hallmark of I/R injury, correlating with the delayed phase of cell death. I/R injury can induce a variety of inflammatory mediators, including interleukin-1 beta (IL-1β), interleukin-6 (IL-6), and tumor necrosis factor alpha (TNFα) in the retina [8-10]. Through phagocytic cells of the innate nonspecific immune system, the inflammatory response is aggravated in the cells post-ischemia injury. The appearance of necrotic cells and the abundance of necrotic factors mediate inflammatory stress, which lead to additional damage after I/R injury [11,12].

Echinacoside (ECH), a natural phenylethanoid found in many medicinal plants, is the principal constituent of the phenylethanoid glycosides isolated from the traditional Chinese herb *Cistanche salsa* [13,14]. Interestingly, recent studies have shown that ECH has protective effects in a

Correspondence to: Zhenzhen Zhang, Department of Ophthalmology, Shanghai Ninth People's Hospital, Shanghai Jiao Tong University School of Medicine, No 639 ZhiZaoJu Road, Shanghai 200011, China; Phone:+86-21-23271699; FAX: +86-02163136856; email: zzz1982.happy@163.com, jannetlee1300@163.com

mouse model of Parkinson disease (PD) induced by 1-methyl-4-phenyl-1,2,3,6-tetrahydropyridine (MPTP) [15]. ECH also attenuates neuroblastoma cell apoptosis induced by TNFα and 6-hydroxydopamine in vitro [16]. However, the mechanism by which ECH promotes the survival of retinal ganglion cells under retinal I/R injury is unclear. In this study, we show that ECH preserves the morphology of retinal cells and reduces ROS products post-I/R in the rat retinal high intraocular pressure (HOP) model remarkably. ECH inhibited apoptosis-associated proteins, such as Apaf-1, Parp, and Bad, and inflammatory factors TNFα, IL-1β, and IL-6.

METHODS

Animals: Adult male Wistar rats were acquired from the Shanghai Laboratory Animal Center of the Chinese Academy of Sciences [17]. The animal care conformed to the Association for Research in Vision and Ophthalmology (ARVO) Statement for the Use of Animals in Ophthalmic and Vision Research and was approved by an Animal Welfare Committee (AWC). The study was masked. The animals were housed in cages with a 12 h:12 h light-dark cycle, at 55%–60% humidity, and temperatures of 23–25 °C. ECH (20 mg/kg) was dissolved in 0.9% normal saline (Sigma-Aldrich, St. Louis, MO) or normal saline as a vehicle control delivered by daily intragastric administration. Rats (total=168) were randomly divided into four groups: sham, sham plus ECH, I/R plus vehicle, and I/R plus ECH. ECH was administered 7 days before the onset of retina ischemia until the day of scarification after 24 h or 7 days. The animals were anesthetized intraperitoneally with 1% pentobarbital sodium (Sigma). Corneal analgesia was achieved using one or two drops of 0.4% oxybuprocaine hydrochloride. Pupil dilatation was maintained with 0.5% tropicamide and 0.5% phenylephrine. Body temperature was maintained at 36.5–37 °C using a heating blanket. Retinal ischemia was induced by increasing the intraocular pressure to 110 mmHg for 45 min [18]. Right eyes were used in all experiments only. After the pupil was dilated, the anterior chamber of the eye was cannulated with a 30-gauge needle connected to a bottle containing normal saline. The intraocular pressure (IOP) was raised to 110 mmHg by lifting the bottle to 150 cm above the eye, and retinal ischemia was confirmed by observing whitening of the iris and loss of the red reflex of the retina. After 45 min of ischemia, the cannulating needle was removed and the intraocular pressure normalized. A sham procedure was performed without the elevation of the container in the control eyes.

Histopathologic examination: Rats (n=6 in each group) were euthanized using an overdose of pentobarbital (intravenously 60–100 mg/kg of bodyweight) at 7 days after the I/R injury, and the eyeballs were enucleated and fixed in 4% paraformaldehyde for 24 h at 4 °C. The fixed retinal tissues were embedded in paraffin, and 5 µm sections were cut through the optic disc. The sections were stained with hematoxylin and eosin. A light microscope (Leica, Heidelberg, Germany) was used for the histopathological evaluation of the tissue sections. Color micrographs were obtained at 400X magnification. Previous studies demonstrated that the changes in the retinal layer thickness accurately reflected the changes in cell number, according to Hughes' reports [19]. We measured different layer thicknesses to quantify the degree of cell loss to measure the ischemic damage in the rat retina. The thicknesses of the entire retina (between the inner limiting membrane and the pigment epithelium), the outer nuclear and the outer plexiform layers (pooled as the outer retinal layers, ORL), the inner nuclear layer (INL), and the inner plexiform layer (IPL) were measured. The measurements (400X) were made 0.5 mm dorsal and ventral from the optic disc. The number of cells in the ganglion cell layer (GCL) was calculated using the linear cell density (cells per 200 µm). For each eye, three measurements at adjacent locations in each hemisphere were made, and the six measurements were averaged. The mean of six eyes was recorded as the representative value for each group.

Retrograde RGC labeling: Deeply anesthetized rats (see above; n=6 in each group) were placed in a stereotactic apparatus (Stoelting, Kiel, Germany), and the skin overlying the skull was cut open. The lambda and bregma sutures served as landmarks for drilling four holes. FG (Biotium, Hayward, CA) was injected (8 µl of 4% FG in distilled H_2O) in the superior colliculus and lateral geniculate bodies [20-22]. To allow for the retrograde transport of FG, the animals were kept for 6 days before further experimentation.

RGC quantification: Animals were anesthetized with halothane (5% for induction, 0.8%–1.0% for maintenance) in 70% N_2O/30% O_2 and perfused transcardially with 4% glutaraldehyde [23]. The eyeballs (n=6 in each group) were removed, and retinal tissues were harvested immediately and placed carefully on a nitrocellulose membrane with the ganglion cell layer on top. After the vitreous body was removed, retinas were fixed in 4% paraformaldehyde for 1 h. The densities of the FG-positive retinal ganglion cells (RGCs) were determined in a blind fashion using fluorescence microscopy (Zeiss 510, Jena, Germany). Briefly, we photographed three standard square areas (0.200 × 0.200 mm=0.040 mm^2) located 1, 2, and 3 mm from the optic disc in the central region of each retinal quadrant. For each retina, the total area evaluated was 0.48 mm^2 (12.0 × 0.04 mm^2), which represents approximately 1% of the rat retina (assuming an average

area per retina of approximately 50 mm^2 in rats [24]). To determine cells/mm^2, we calculated the cell density as the number of analyzed cells/0.04 mm^2 × 25. Data are given as the mean RGC densities (cells/mm^2) ± standard error of the mean (SEM).

TUNEL staining: Seven days after I/R, rats were euthanized by using an overdose of pentobarbital (intravenously 60–100 mg/kg of bodyweight). Enucleated eyeballs (n=6 in each group) were fixed in 4% paraformaldehyde for 24 h at 4 °C. Fixed retinal tissues were embedded in paraffin, and 5 µm sections thick cut through the optic disc. All according to the manufacturers' protocols, paraffin-embedded retinal tissue sections were deparaffinized, rehydrated, and pretreated with proteinase K. Terminal deoxynucleotidyl transferase-mediated dUTP nick end-labeling (TUNEL) assays were performed using an in situ cell death-detection kit, TMR Red (Roche, Lewes, UK). Slides were mounted in VECTASHIELD fluorescence mounting medium with 4′,6-diamidino-2-phenylindole (DAPI; Sigma) for nuclear staining and visualized under a laser scanning confocal microscope system (Zeiss 510, Jena, Germany). The apoptotic cells within the retina fluoresced red; Zeiss 4.6 version software was used for image collection.

Optic nerve histology and transmission electron microscopy: Seven days after ischemia, the rats were anesthetized (see above; n=6 in each group) and transcardially perfused with 4% glutaraldehyde. The eyeballs with the optic nerves were removed and immersed in 4% glutaraldehyde for 24 h at 4 °C. Optic nerves segments 2 mm from the back of the globe were dissected, washed, postfixed, impregnated with uranyl acetate, and embedded in Epon (Head biotechology, Beijing, China). Semithin sections were cut and stained with toluidine blue (n=6 in each group). The stained sections were photographed using a light microscope (Leica, Heidelberg, Germany).

For the transmission electron microscopy (TEM) assay, rats were transcardially perfused with 4% glutaraldehyde under anesthesia (see above), and the optic nerves were dissected carefully and placed in fixative (approximately 20 ml of 2.5% glutaraldehyde and 2.0% paraformaldehyde in 0.15 M cacodylate buffer) overnight. Then, the optic nerves were postfixed in 1% osmium tetroxide, stained in 2% uranyl acetate, dehydrated in ethanol and acetone, and embedded in epoxy resin. Ultrathin sections were cut perpendicular to the long axis of the optic nerve on an ultramicrotome (LKB-1, Bromma, Sweden), stained with lead citrate, and observed using a transmission electron microscope (JEM-1230, Peabody, MA) equipped with a digital camera.

Determining the MDA level and SOD, GSH-Px, and CAT activity: Twenty-four hours after ischemia, the animals were euthanized using an overdose of pentobarbital (intravenously 60–100 mg/kg of bodyweight), and the retinas were immediately extracted (n=6 in each group). The retina samples were prepared as a 10% homogenate in 0.9% saline according to weight using a homogenizer on ice. Then, the homogenate was sedimented at 2,000 × *g* for 10 min, and the supernatant was collected and diluted.

MDA levels were determined using Draper and Hadley's double heating method [25]. MDA, the end product of fatty acid peroxidation, reacts with thiobarbituric acid (TBA) to form a colored complex. Briefly, 2.5 ml of TBA solution (100 g/l) was added to 0.5 ml of homogenate in each centrifuge tube, and then the tubes were placed in boiling water for 15 min. After cooling with flowing water, the tubes were centrifuged at 1,000 × *g* for 10 min, 2 ml of the supernatant were added to 1 ml of TBA solution (6.7 g/l), and the tube was placed in boiling water for another 15 min. After cooling, the amount of thiobarbituric acid-reactive species (TBARS) was measured at 532 nm. The MDA concentration was calculated from the absorbance coefficient of the MDA–TBA complex. Data are expressed as nanomoles per gram (nmol/g) tissue protein.

The total (Cu/Zn and Mn) SOD activity was determined through the inhibition of nitrotetrazolium blue (NTB) reduction by the xanthine/xanthine oxidase system as a superoxide generator, as previously reported by Sun et al. [26]. The activity was assessed in the supernatant after the 1.0 ml ethanol/chloroform mixture (5/3, v/v) was added to the same volume of sample and separated for 15 min at 3,000 × *g*. The production of formazan was determined by absorbance at 560 nm. One unit of SOD was defined as the amount of protein that inhibited the rate of NTB reduction by 50%.

GSH-Px activity was measured with Paglia and Valentine's method [27]. The enzymatic reaction in the tube that contained reduced nicotinamide adenine dinucleotide phosphate, reduced glutathione, sodium azide, and glutathione reductase was initiated by the addition of H_2O_2, and the change in absorbance at 340 nm was monitored with spectrophotometry.

CAT activity was measured with Cohen's method [28]. The principle of the assay was based on the determination of the rate constant (s^{-1}, k) of H_2O_2 decomposition. The rate constant of the enzyme and protein levels was determined by measuring the absorbance change per minute and the Lowry method [29], respectively.

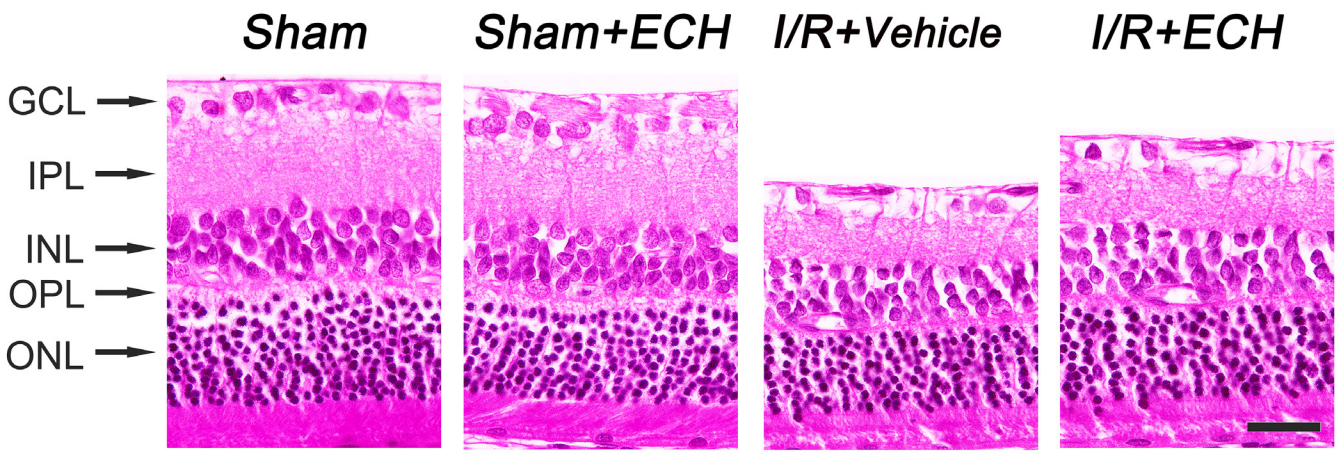

Figure 1. Representative photographs of rat retinas 7 days after I/R without or with ECH. **A**, **B**: In the sham group and the sham plus echinacoside (ECH) group, the GCL and the INL were clear and well organized. **C**, **D**: Seven days after the ischemia/reperfusion (I/R) injury, the INL in the I/R plus vehicle group was obviously thinner, and the number of GCL cells had decreased, whereas in the I/R plus ECH group, the retina was more normal in structure, with a thicker INL than in the I/R plus vehicle group. GCL, ganglion cell layer; INL, inner nuclear layer; IPL, inner plexiform layer; OPL, outer plexiform layer; ONL, outer nuclear layer. Scale bar: 20 µm.

Total RNA extraction and qPCR: Retinas were harvested (n=6 per group) 24 h after ischemia. To evaluate the influence of treatments on mRNA, quantitative real-time PCR (qPCR) was performed on retinal tissues. Total RNA was extracted from tissues using TRIzol Reagent (Invitrogen, Carlsbad, CA). cDNA synthesis was performed with 1 µg of total RNA and a Sprint RT Complete-Double PrePrimed Kit (Clontech, Mountain View, CA). One microliter of each cDNA (dilution 1:10) was used as the template in the qPCR assays, performed in triplicate of three biologic replicates on Mastercycler RealPlex (Eppendorf, Haupauge, NY) by using the SYBR Green qPCR Premix (Clontech). The cycling parameters consisted of 95 °C for 10 min, followed by 40 cycles of 95 °C for 15 s, 60 °C for 1 min, and 72 °C for 30 s. The relative levels of target mRNA expression were calculated using the $2^{-\Delta\Delta Ct}$ method. The primers used were Apaf-1 forward (5′-ACA CCT TCT TGG ACG ACA G-3′) and reverse (5′-AGC AGG CAT GGT AAA CAG C-3′) primers; Parp forward (5′-GCA GAG TAT GCC AAG TCC AAC AG-3′) and reverse (5′-ATC CAC CTC ATC GCC TTT TC-3′) primers; Bad forward (5′-CAG GCA GCC AAT AAC AGT-3′) and reverse (5′- CCA TCC CTT CAT CTT CCT C-3′) primers; and β-actin forward (5′-TCG TGC GTG ACA TTA AGG AGA AG-3′) and reverse (5′- GTT GAA GGT AGT TTC GTG GAT GC-3′) primers.

Standard curves were generated from known quantities for each of the target genes of linearized plasmid DNA. Ten times dilution series were used for each known target, which were amplified with qPCR. The linear regression line for a nanogram of DNA was determined from relative fluorescent units at a threshold fluorescence value (Ct) to quantify the gene target from the cell extracts by comparing the relative fluorescent units at the threshold fluorescence to the standard curve, normalized by the simultaneous amplification of β-actin.

Table1. Thickness of the retinal layers and GCL cell count at 7 days after I/R.

Group	Thickness (µm)				GCL cell number (cells per 200 µm)
n=6	Entire retina	INL	IPL	ORL	
Sham	144.23±3.69	28.42±1.92	27.24±1.94	57.24±3.61	17.09±1.41
Sham/ECH	143.59±3.84	27.93±1.74	28.05±1.81	57.50±2.91	17.17±1.62
I/R/Vehicle	100.73±3.61[a]*	16.95±1.06[a]*	13.01±0.92[a]*	30.81±1.50[a]*	7.89±0.83[a]*
I/R/ECH	126.41±3.63 [b]*	21.21±1.26 [b]*	23.52±1.40 [b]*	46.12±4.65 [b]*	12.91±1.61 [b]*

Values are (means ±SE). n=6. Values compared between groups by one-way ANOVA with Dunnett's post-test. a:compared with the ***Sham*** group; b:compared with the ***I/R plus vehicle*** group,*p<0.05 INL, inner nuclear layer; IPL, inner plexiform layer; ORL, outer retinal layers; GCL, ganglion cell layer; I/R, high intraocular pressure induced ischemia/reperfusion injury; ECH, echinacoside.

Enzyme-linked immunosorbent assay: Seven days after ischemia, the animals (n=6 in each group) were euthanized using an overdose of pentobarbital (intravenously 60–100 mg/kg of bodyweight), and the retinas were immediately extracted. The retina samples were prepared as a 10% homogenate in 0.9% saline according to weight using a homogenizer on ice. Then, the homogenate was sedimented at 2,000 × *g* for 10 min, and the supernatant was collected and diluted. The levels of secreted TNFα, IL-1β, and IL-6 in the retinal supernatants were determined with enzyme-linked immunosorbent (ELISA), and the amount of TNFα, IL-1β, and IL-6 released was determined using the TNFα, IL-1β, and IL-6 Emax® ImmunoAssay System following the manufacturer's protocol (Promega, Madison, WI).

Western blotting: Some of the animals were euthanized using a pentobarbital (intravenously 60–100 mg/kg of body at 7 days post-I/R, and the retina tissues were immediately extracted. The tissues were washed with PBS (1X; 120 mM NaCl, 20 mM KCl, 10 mM $NaPO_4$, 5 mM KPO_4, pH 7.4) and homogenized in lysis buffer (Cell Signaling Technology,

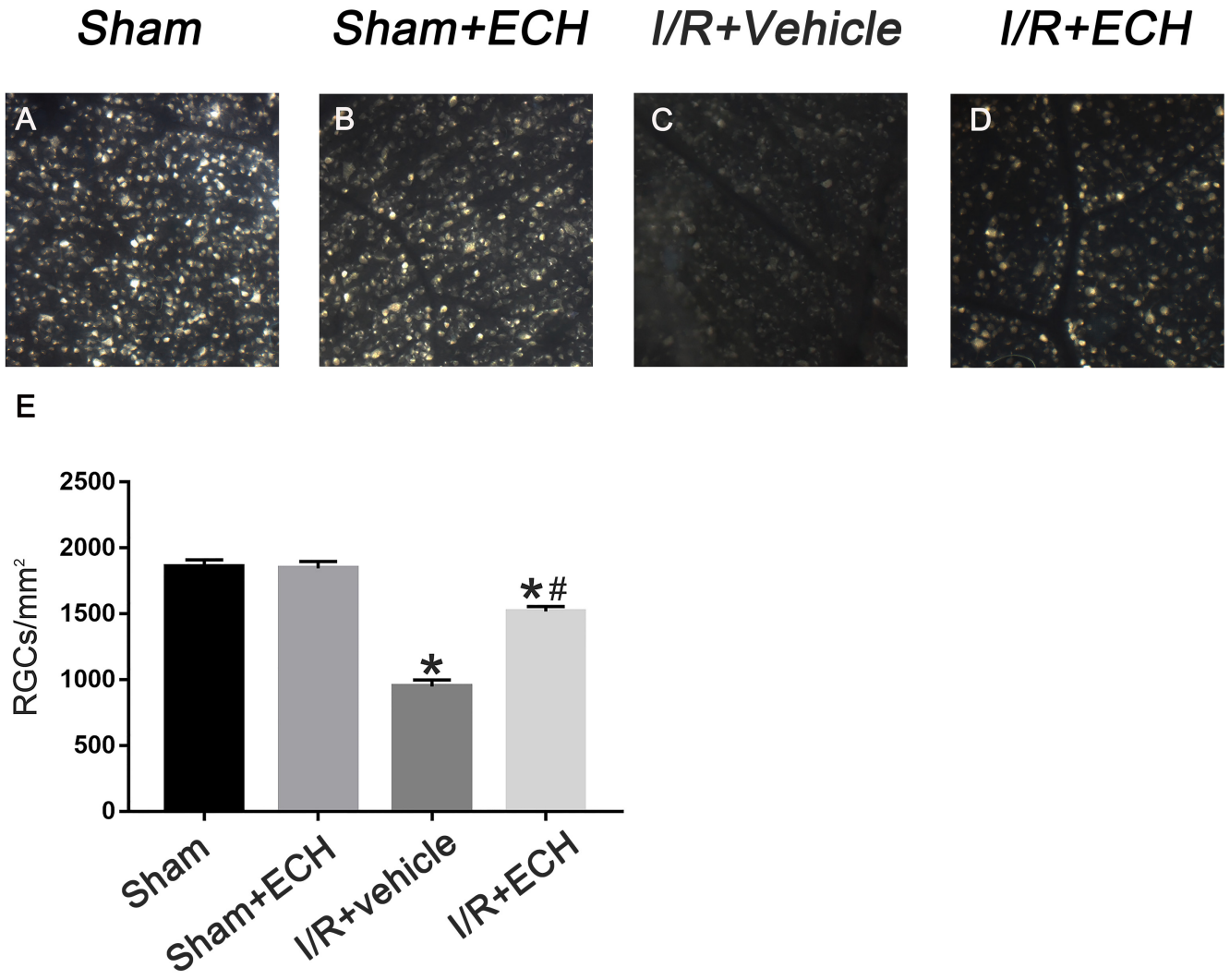

Figure 2. Comparison of RGCs in four treated groups. **A**, **B**: Most retinal ganglion cells (RGCs) stained Fluoro-Gold (FG)-positive 7 days in the sham group and the sham plus echinacoside (ECH) group. **C**: Many RGCs died, and activated microglia cells stained FG-positive after phagocytosis in the retinas of the rats that received vehicle at 7 days after the ischemia/reperfusion (I/R) injury. **D**: In the retinas of the I/R plus ECH group, there were more RGCs stained FG-positive than in the retinas in the I/R plus vehicle group. *p<0.05 versus sham group; #p<0.05 versus I/R plus vehicle group. **E**: The bar graph represents the total number of RGCs in all groups. There was a statistically significant loss, an approximate 31.11% reduction in the number of RGCs in the I/R plus vehicle group with respect to the I/R plus ECH group. Scale bar: 100 µm. *p<0.05.

Beverly, MA) supplemented with protease inhibitors (Roche Applied Science, Indianapolis, IN). The protein concentration was determined with a bicinchoninic acid protein assay reagent kit (Pierce, Rockford, IL). Samples containing 30 mg of protein were electrophoretically separated in 10% polyacrylamide gels containing 0.1% sodium dodecyl sulfate (SDS) and transferred to polyvinylidene difluoride membranes. The membranes were incubated overnight at 4 °C with one of the following primary antibodies: anti-Parp (1:1,000; Stressgen Biotechnologies, Victoria, Canada), anti-Apaf (1:1,000; Cell Signaling Technology), anti-Bad (1:1,000; Santa Cruz Biotechnology, Santa Cruz, CA), and anti-β-actin (1:1,000; Cell Signaling Technology). After the membrane was washed, horseradish peroxidase-conjugated goat anti-rabbit immunoglobulin G (IgG) was added as the secondary antibody, and the membrane was incubated at room temperature for 1 h. Immunoreactive proteins were visualized with enhanced chemiluminescence (ECL; Amersham Pharmacia Biotech, Piscataway, NJ).

Statistical analysis: The experimental data were expressed as mean ± standard deviation (SD). A p value of less than 0.05 was considered statistically significant using multiple analysis of the variance (ANOVA) and the Student–Newman–Keuls test with SPSS 13.0 software (SPSS, Inc., Chicago, IL).

RESULTS

Histopathologic examination: At 7 days after I/R, the overall retinal thickness, number of GCL cells, and thicknesses of the IPL, INL, and ORL in the I/R plus vehicle group were statistically significantly decreased compared with the animals in the sham group ($p<0.05$; Figure 1C), whereas no histopathological differences were found between the sham group and the sham plus ECH group ($p>0.05$; Figure 1A,B).

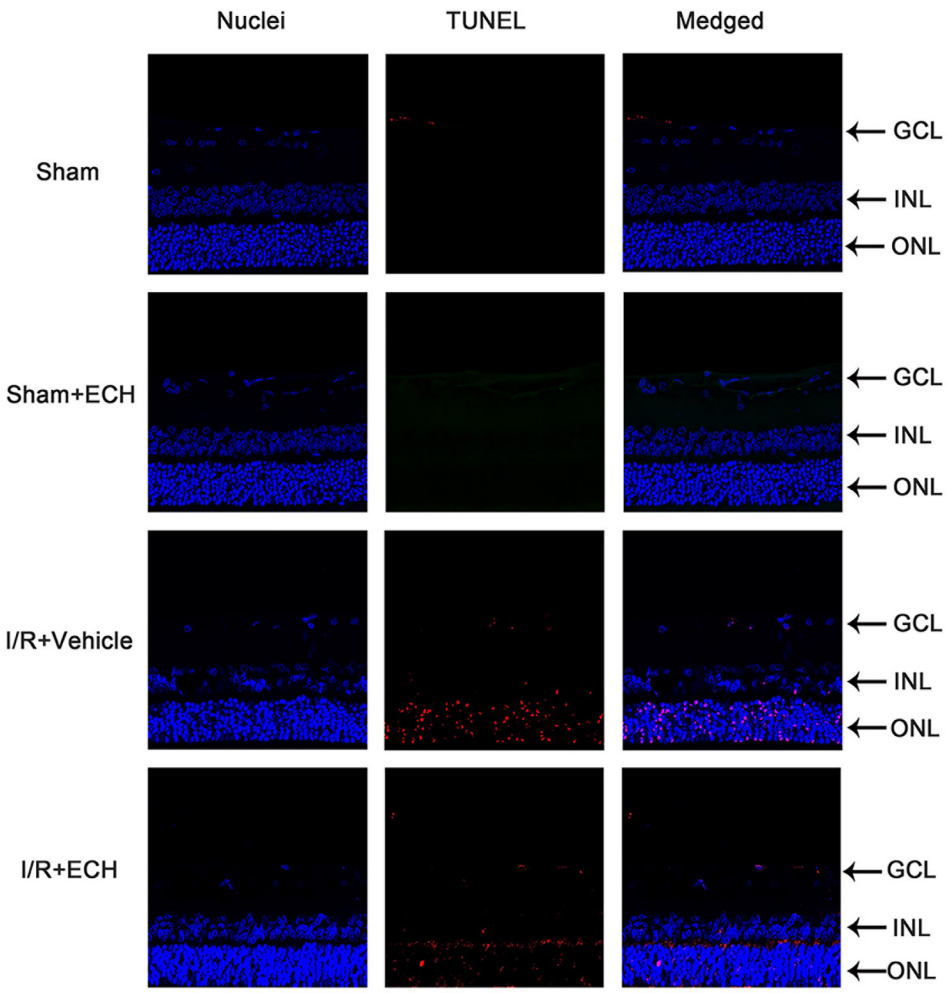

Figure 3. Fluorescence detection of neuronal cell apoptosis at 7 days after I/R. **A**, **B**: No terminal deoxynucleotidyl transferase-mediated dUTP nick end-labeling (TUNEL)-positive cells were seen in the sham group and the sham plus echinacoside (ECH) group. **C**: Abundant red fluorescent nuclei were observed in the ischemia/reperfusion (I/R) plus vehicle rats. **D**: Sparse red fluorescent nuclei were found in the I/R plus ECH rats. GCL, ganglion cell layer; INL, inner nuclear layer; ONL, outer nuclear layer.

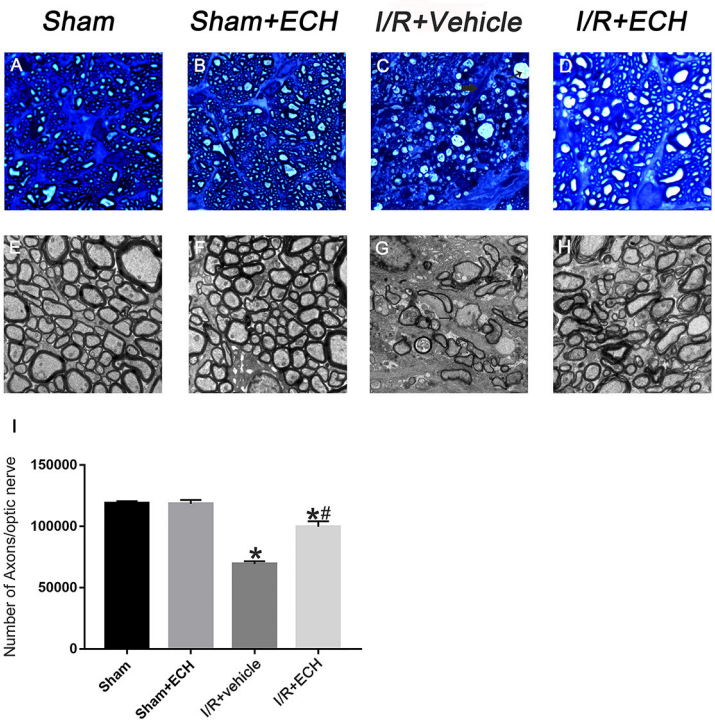

Figure 4. Histological comparison of optic nerves in 4 groups after I/R. **A**, **B**: Optic nerves show tightly packed myelinated axons and thin septae from the sham group and the sham plus echinacoside (ECH) group. **C**: Optic nerves from vehicle-treated animals show disruption of the axon fascicles, severe axonal loss (thin arrow), and increases in connective tissue septa (big arrow). **D**: In the ischemia/reperfusion (I/R) plus ECH group, the preservation of the retinal ganglion cell (RGC) axons was better than in vehicle control, although with a relative increase in the septal connective tissue. Scale bar: 200 µm. Electron micrographs of transverse sections of optic nerves from the sham group, the I/R plus vehicle group, and the I/R plus ECH group post-insult. **E**, **F**: Optic nerves show an orderly arrangement of the myelin sheath in the axons in the sham group and the I/R plus ECH group. **G**: In the I/R plus vehicle group, myelinated nerve fibers are scarce and irregularly arranged, with distinct axonal damage, seen as swollen, collapsed axons (thin arrow), condensed electron opaque axoplasm (big arrow). **H**: In the I/R plus ECH group, ECH attenuated axon damage, although some condensed electron opaque axoplasm and detachment of the myelin lamellae from the cytoplasmic membrane are also observed. Scale bar: 4 µm. **I**: The bar graph represents the total number of axons in all groups. There was a statistically significant loss, approximately a 39.31% reduction in the number of axons in the I/R plus vehicle group with respect to the sham group (*$p<0.05$), and there was an approximately 25.47% reduction in the number of axons in the I/R plus vehicle group compared with the I/R plus ECH group ($^{\#}p<0.05$).

The overall thickness of the retina in the I/R plus vehicle group was reduced by 24% compared with the sham group (100.73±3.6100 versus 144.23±3.6900 µm). The retinal layers in order of reduced magnitude were the IPL, INL, and ORL, which were reduced by 41%, 52%, and 46%, respectively; the GCL density was reduced by 54% in the I/R plus vehicle group (Table 1, Figure 1C). In the I/R plus ECH group, ECH clearly protected the retina against retinal ischemic damage; the retina appeared more normal with thicker inner retinal layers (INL and IPL) than in the I/R plus vehicle group (Figure 1D). Measurements of the layer thicknesses and the GCL cell number quantitatively confirmed the protective effect of ECH (Table 1). The overall retinal thickness in the I/R plus ECH group was statistically significantly greater than that in the I/R plus vehicle group ($p<0.05$). Approximately 60% of the loss caused by I/R was prevented. The IPL and INL thicknesses and the GCL density in the I/R plus ECH group were also greater than those in the I/R plus vehicle group ($p<0.05$).

ECH protected RGCs from death after I/R: ECH statistically significantly delayed cell death in the retina after I/R. In the I/R plus ECH group, most RGCs were FG-positive 7 days post-I/R compared with the I/R plus vehicle group (Figure 2D), while many ischemic RGCs that received vehicle died (Figure 2C). Seven days after I/R, the ECH-treated group had 1,624±54.00 RGC/mm^2, whereas those treated with vehicle had 1,006±63.00 RGC/mm^2 ($p<0.001$). In the sham group eyes, 1,859±59.00 RGC/mm^2 were counted (Figure 2A), and in the sham plus ECH eyes, 1,872+63.00 RGC/mm^2 were counted (Figure 2B).

TUNEL staining: Fluorescent detection of retinal cell apoptosis was performed 7 days after I/R (Figure 3). For rats in the sham group and the sham plus ECH group (Figure 3A,B), the retina cell nuclei were negative for TUNEL staining. Abundant red fluorescent retinal cell nuclei were found within the inner nuclear, outer nuclear, and ganglion cells in the I/R-plus vehicle group (Figure 3C). In contrast, in the I/R plus ECH group (Figure 3D), only a few red fluorescent nuclei were found on TUNEL staining of the rat retinas.

Table 2. Difference of MDA level and SOD, GSH-Px, and CAT activities.

Group n=6	Average oxidative parameters			
	MDA (nmol/g)	SOD (u/g)	CAT (u/g)	GSH-px (u/g)
Sham	21.41±0.96	0.82±0.01	1.81±0.22	23.21±1.76
Sham/ECH	20.72±2.01	0.83±0.03	1.87±0.06	23.79±0.58
I/R/vehicle	38.21±1.53 a*	0.63±0.06 a*	1.20±0.15 a*	15.84±1.52 a*
I/R/ECH	28.56±1.04 b*	0.78±0.04 b*	1.55±0.05 b*	19.03±0.92 b*

Values are (means ±SE). n=6. Values of retinal malondialdehyde (MDA), superoxide dismutase (SOD), catalase (CAT), and glutathione peroxidase (GSHPx) were compared between groups using one-way ANOVA with Dunnett's post-test. a:compared with the Sham group; b:compared with the I/R plus vehicle group,*p<0.05

ECH-mediated neuroprotection in axonal damage after ischemia:

Optic nerve histology—There were similarly intact, myelinated RGC axons in the sham group and the sham plus ECH group (Figure 4A,B,I). The RGC axon loss was statistically significant in the I/R plus vehicle group (Figure 4C,I). In contrast, in the I/R plus ECH group, the preservation of RGC axons was better than in the I/R plus vehicle group, although a relative increase in septal gliosis was observed (as shown in Figure 4D,I).

Transmission electron microscopy—In the sham group and the sham plus ECH group, electron microscopic examination revealed an orderly arrangement of the myelin sheath and intact mitochondria in the axons (Figure 4E,F). However, in the I/R plus vehicle group, myelinated nerve fibers were scarce and arranged irregularly, with distinct axonal damage, seen as swollen, collapsed axons, condensed electron opaque axoplasm, and detachment of the myelin lamellae from the cytoplasmic membrane. In addition, several swollen mitochondria were seen (Figure 4G). ECH statistically significantly attenuated the axon damage post-insult, although some

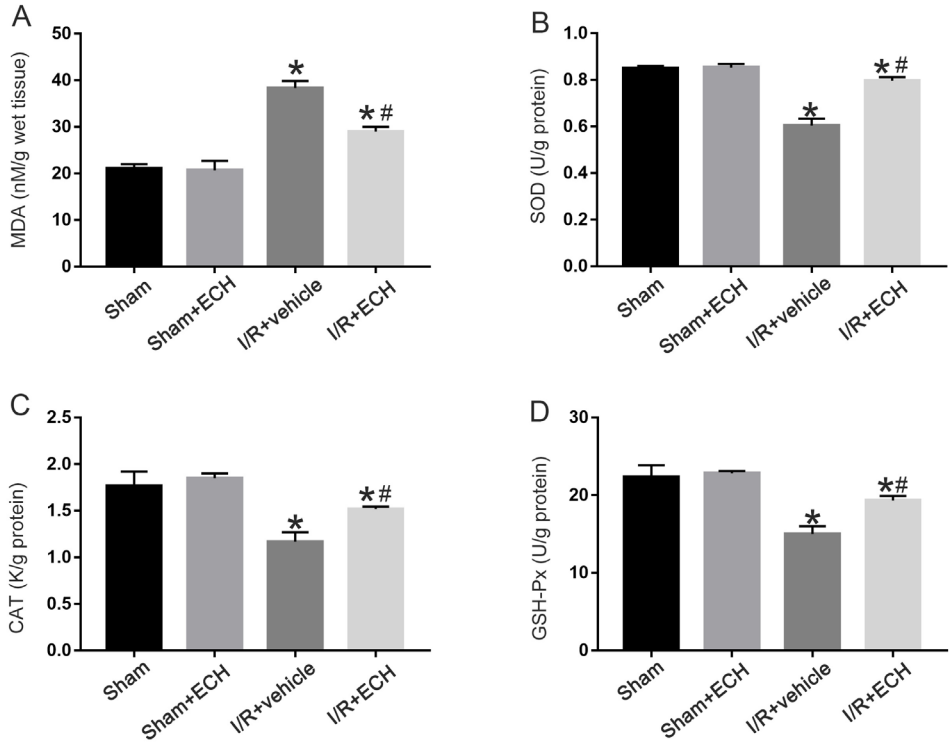

Figure 5. Difference in MDA levels and SOD, GSH-Px, and CAT activities in the retina 24 h after I/R. **A**: Malondialdehyde (MDA) levels in the ischemia/reperfusion (I/R) plus vehicle group and the I/R plus echinacoside (ECH) group became statistically significantly higher than those of the sham group and the sham plus ECH group ($p<0.05$). The MDA level in the I/R plus ECH group was higher than that of the sham group but was statistically significantly lower than that of the I/R plus vehicle group ($p<0.05$). **B**–**D**: The superoxide dismutase (SOD), catalase (CAT), and glutathione peroxidase (GSH-Px) activity in the I/R plus vehicle group and the I/R plus ECH group became statistically significantly lower than that of the sham group ($p<0.05$). The activities in the sham group plus ECH group were statistically significantly higher than those in the I/R plus vehicle group ($p<0.05$). *$p<0.05$ versus the sham group; #$p<0.05$ versus the I/R plus vehicle group.

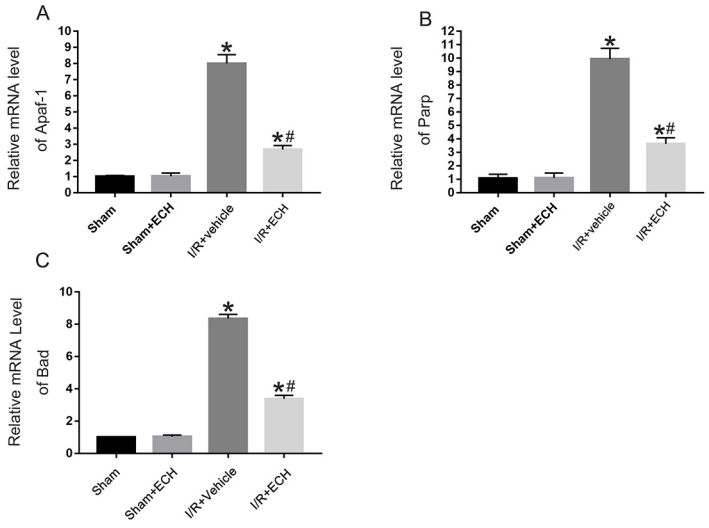

Figure 6. ECH treatment reduced activation of Parp, Apaf-1, and Bad mRNA in retinas 7 days after I/R. **A**–**C**: Quantitative real-time PCR (qPCR) shows statistically significant activation of Parp, Bad, and Apaf-1 in the retinas after ischemia/reperfusion (I/R) injury; echinacoside (ECH) treatment reduced these effects. Histograms represent the mean ± standard error of the mean (SEM) of apoptotic mRNA levels in the retinas of all groups. *p<0.01 versus the sham group; #p<0.01 versus the I/R plus vehicle group.

condensed electron opaque axoplasm and detachment of the myelin lamellae from the cytoplasmic membrane were also observed (Figure 4H).

MDA levels and SOD, GSH-Px, and CAT activity: Twenty-four hours after I/R, the MDA levels in the retinas of the I/R plus vehicle group and the I/R plus ECH group were statistically significantly higher than those in the sham

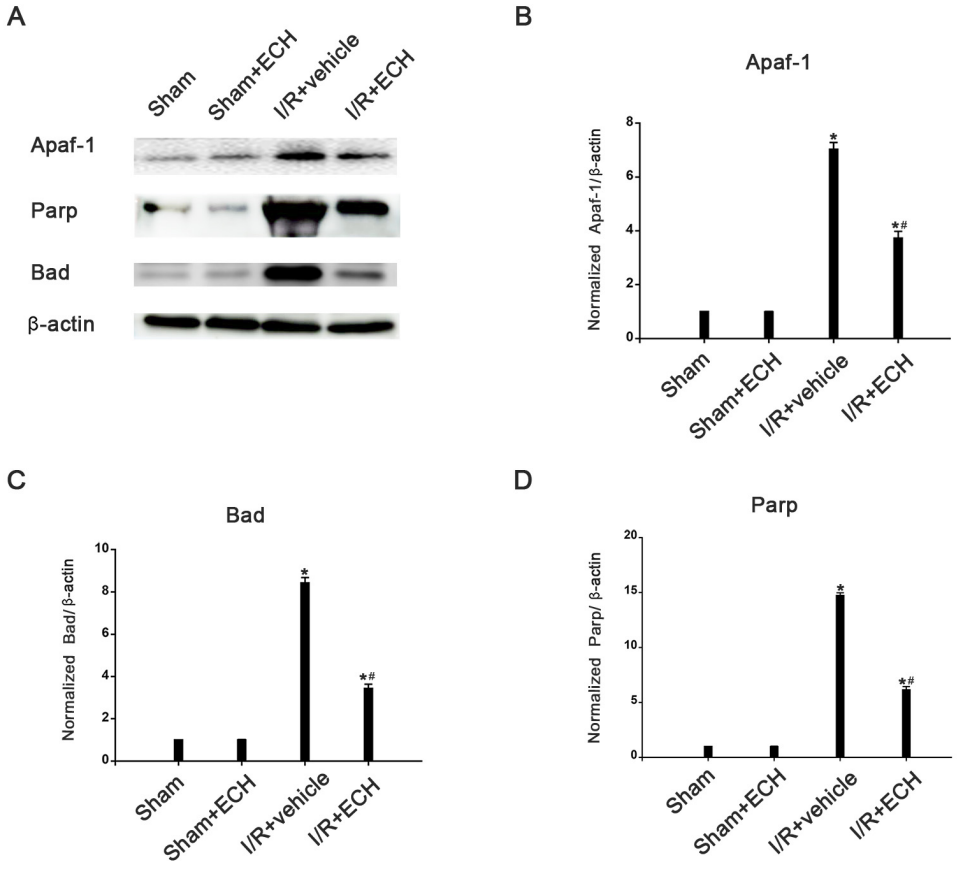

Figure 7. ECH treatment reduced release of Parp, Apaf-1, and Bad in the retina 7 days post-I/R. **A**: western blotting shows statistically significant activation of Parp, Apaf-1, and Bad in the retinas after ischemia/reperfusion (I/R) injury; echinacoside (ECH) treatment reduced these effects. **B**–**D**: Histograms represent the mean ± standard error of the mean (SEM) of the Parp, Apaf-1, and Bad protein levels in the retinas of all groups.*p<0.01 versus the sham group; #p<0.01 versus the I/R plus vehicle group.

group (p<0.05). The MDA levels in the retinas in the sham group and the sham plus ECH group were similar (p>0.05), and the levels in the retinas in the I/R plus ECH group were statistically significantly lower than in the retinas in the I/R plus vehicle group (p<0.05; Figure 5A, Table 2).The activity of SOD, GSH-Px, and CAT was similar between the sham group and the sham plus ECH group (p>0.05), and was statistically significantly higher than that in the retinas in the I/R plus vehicle group (p<0.05). However, the activities of these enzymes in the retinas of the I/R plus ECH group were statistically significantly higher than those in the retinas in the I/R plus vehicle (p<0.05; Figure 5B–D, Table 2).

ECH suppresses ROS-induced gene expression after I/R injury: We used qPCR and western blotting to analyze the expression of Apaf-1, Parp, and Bad in the retinal tissues and found that I/R statistically significantly enhanced the release of Apaf-1, Parp, and Bad (Figure 6A–C, Figure 7A–D). However, ECH partially reversed the phenomenon.

Suppressed expression of inflammatory factors in the retina by ECH: ELISA showed that intracellular TNFα, IL-1β, and IL-6 are upregulated after I/R injury (Figure 8A–C). Of note, treatment with ECH attenuated the expression of intracellular TNFα, IL-1β, and IL-6 post-insult. Taken together, the results show that ECH statistically significantly suppressed expression of inflammatory factors in the injured retina.

DISCUSSION

The rat transient IOP elevation model mimics circulatory disorders of the retina resulting from elevated intraocular pressure, followed by compression of retinal blood vessels, which, in turn, leads to impaired blood flow. The following natural reperfusion induces strong oxidative stress, which induces I/R injury and risk of retinal artery occlusion and glaucoma [30-32]. Oxidative stress, an imbalance that favors prooxidant over antioxidant factors, leads to cellular damage in retinal I/R [1,33,34]. As MDA is a naturally occurring product of lipid peroxidation, a process in which unsaturated fat-soluble substances (lipids) are oxidized to form radicals, the MDA level reflects the severity of the cellular damage [31]. In addition, ROS can be scavenged by antioxidant enzymes, including SOD, CAT, and GSH-Px. Therefore, the activity of those enzymes may help in evaluating the antioxidant enzyme status [4,35,36]. In this study, we found ECH dramatically protected retinal cells against I/R injury, indicated by a reduction in histological damage. We also found that ECH improved the antioxidative stress parameters and prevented inflammatory factor release in the rat retina I/R model. ECH also attenuated cell-death-associated gene activation, which suggests mechanisms of protection by ECH.

In this study, application of ECH did not change the level of antioxidative enzymes (SOD, CAT, and GSH-Px) and lipid peroxidation (MDA) in the sham plus ECH group compared with the sham group, ruling out the possibility of a direct effect of ECH on inducing stronger oxidative stress responses. However, I/R led to a significant increase in lipid peroxidation (MDA) with impaired activity of antioxidative enzymes (SOD, CAT, and GSH-Px) activity in the retina, whereas ECH prevented lipid peroxidation (decreased MDA levels) and induced activation of antioxidant enzymes (SOD, CAT, and GSH-Px) in the retina, accompanied by suppression of inflammatory factors TNFα, IL-1β, and IL-6, in accordance

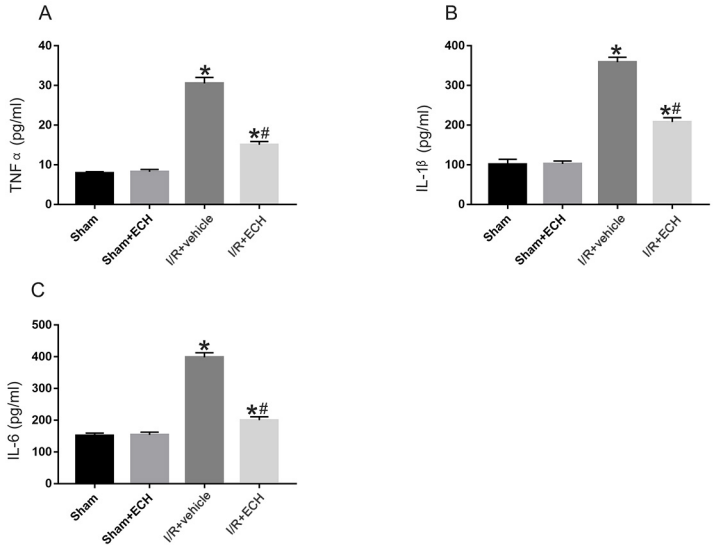

Figure 8. ECH administration attenuated release of TNFα, IL-1β, and IL-6 in the retina 7 days after I/R. **A**–**C**: Enzyme-linked immunosorbent assay (ELISA) shows statistically significant release of TNFα, IL-1β, and IL-6 in the retinas after ischemia/reperfusion (I/R) injury; echinacoside (ECH) treatment statistically significantly reduced these effects. Histograms represent the mean ± standard error of the mean (SEM) of the tumor necrosis factor-α (TNFα), interleukin-1 beta (IL-1β), and IL-6 protein levels in the retinas of all groups.*p<0.01 versus the sham group; #p<0.01 versus the I/R plus vehicle group.

with previous studies [37,38]. These results suggested the protection of ECH against I/R injury is due to modulation of the response to oxidative stress and the release of inflammatory factors.

Recently, ECH has been identified as a potent antioxidant in the central nervous system [39]. Tubuloside B, one of the phenylethanoids isolated from the stems of *Cistanche salsa*, exerts neuroprotection to antagonize TNFα-induced apoptosis in SH-SY5Y cells and may be useful in treating neurodegenerative diseases [16]. These studies showed the neuroprotective effects of echinacoside on 4-aminopyridine-evoked glutamate release in rat cerebrocortical nerve terminals (synaptosomes), which was associated with reduced voltage-dependent Ca^{2+} entry and subsequent suppression of protein kinase C activity [39]. Zhao et al. found that echinacoside protects against MPP^{+}-induced neuronal apoptosis via regulation of the ROS/ATF3/CHOP change to: reactive oxygen stress (ROS) /activating transcription factor 3(ATF3)/C/EBP homologous protein (CHOP) pathway [15], and it has been reported echinacoside stimulates cell proliferation and prevents cell apoptosis in intestinal epithelial MODE-K cells by upregulation of transforming growth factor-β1 expression [40]. Zhang et al. reported that echinacoside protects nigrostriatal dopaminergic pathways against 6-OHDA-induced endoplasmic reticulum stress by reducing the accumulation of seipin [41]. Cistanoside A possesses antiosteoporotic activity in ovariectomized mice via TRAF6-mediated NF-kappaB inactivation and PI3K/Akt activation, to promote bone formation and prevent bone resorption [42]. It has been suggested that apoptosis and necrosis are involved in I/R-induced cell damage, and apoptosis plays a major role [2]. In this study, qPCR analysis of Apaf-1, Parp, and Bad revealed that abundant release of proapoptotic factors was induced by I/R insult but attenuated by the administration of ECH. This demonstrated that ECH could prevent apoptosis of retinal cells, and ELISA of TNFα, IL-1β, and IL-6 showed that ECH has anti-inflammatory effects in retinas under I/R injury. As massive numbers of ROS, which trigger apoptosis [3], are generated during I/R [5], the antiapoptosis mechanism of ECH in I/R-induced retinal cell damage may also be due to its antioxidant and anti-inflammatory potential.

Previous studies suggested that a phenylethanoid glycoside–rich extract of *Cistanche deserticola* (PhG-RE), a well known natural antioxidant-based active constituent, may protect against oxidative stress in the reperfused myocardium and play a significant role in the inhibition of apoptotic pathways [43]. *Cistanches Herba* extract increased neuronal cell differentiation, neurite length, and synapse formation in the mouse hippocampus through upregulating nerve growth factor (NGF), and statistically significantly enhanced learning and memory [44].

In conclusion, this study demonstrated that ECH, a principal constituent of the phenylethanoid glycosides isolated from the traditional Chinese herb *Cistanche salsa,* protects retinal cells against I/R-induced retinal damage. The protective effect of ECH appears to be due to the inhibition of oxidative stress, inflammation, and apoptosis. The results suggest that ECH plays a role in neuroprotection for the treatment of I/R-related retinal diseases.

ACKNOWLEDGMENTS

This study was supported by a grant from National Natural Science Foundation of China (Grant No.81300779) and a grant from The Science and Technology Commission of Shanghai (Grant No.17DZ2260100).

REFERENCES

1. Osborne NN, Casson RJ, Wood JP, Chidlow G, Graham M, Melena J. Retinal ischemia: mechanisms of damage and potential therapeutic strategies. Prog Retin Eye Res 2004; 23:91-147. [PMID: 14766318].

2. Buchi ER. Cell death in the rat retina after a pressure-induced ischaemia-reperfusion insult: an electron microscopic study. I. Ganglion cell layer and inner nuclear layer. Exp Eye Res 1992; 55:605-13. [PMID: 1483506].

3. Szabo ME, Droy-Lefaix MT, Doly M, Carre C, Braquet P. Ischemia and reperfusion-induced histologic changes in the rat retina. Demonstration of a free radical-mediated mechanism. Invest Ophthalmol Vis Sci 1991; 32:1471-8. [PMID: 2016129].

4. Agardh CD, Gustavsson C, Hagert P, Nilsson M, Agardh E. Expression of antioxidant enzymes in rat retinal ischemia followed by reperfusion. Metabolism 2006; 55:892-8. [PMID: 16784960].

5. Di Mascio P, Murphy ME, Sies H. Antioxidant defense systems: the role of carotenoids, tocopherols, and thiols. Am J Clin Nutr 1991; 53:194S-200S. [PMID: 1985387].

6. Ji D, Li GY, Osborne NN. Nicotinamide attenuates retinal ischemia and light insults to neurons. Neurochem Int 2008; 52:786-98. [PMID: 17976861].

7. Zhang Z, Qin X, Zhao X, Tong N, Gong Y, Zhang W, Wu X. Valproic acid regulates antioxidant enzymes and prevents ischemia/reperfusion injury in the rat retina. Curr Eye Res 2012; 37:429-37. [PMID: 22458760].

8. Franks WA, Limb GA, Stanford MR, Ogilvie J, Wolstencroft RA, Chignell AH, Dumonde DC. Cytokines in human intraocular inflammation. Curr Eye Res 1992; 11:187-92. [PMID: 1424744].

9. Kaur C, Foulds WS, Ling EA. Hypoxia-ischemia and retinal ganglion cell damage. Clin Ophthalmol 2008; 2:879-89. [PMID: 19668442].

10. Zheng L, Gong B, Hatala DA, Kern TS. Retinal ischemia and reperfusion causes capillary degeneration: similarities to diabetes. Invest Ophthalmol Vis Sci 2007; 48:361-7. [PMID: 17197555].

11. Schwartz M. Neuroprotection as a treatment for glaucoma: pharmacological and immunological approaches. Eur J Ophthalmol 2001; 11:S7-11. [PMID: 11592535].

12. Meldrum DR, Dinarello CA, Cleveland JC Jr, Cain BS, Shames BD, Meng X, Harken AH. Hydrogen peroxide induces tumor necrosis factor alpha-mediated cardiac injury by a P38 mitogen-activated protein kinase-dependent mechanism. Surgery 1998; 124:291-6. [PMID: 9706151].

13. Tu PF, Wang B, Deyama T, Zhang ZG, Lou ZC. Analysis of phenylethanoid glycosides of Herba cistanchis by RP-HPLC. Yao Xue Xue Bao 1997; 32:294-300. [PMID: 11499033].

14. Wang YM, Zhang SJ, Luo GA, Hu YN, Hu JP, Liu L, Zhu Y, Wang HJ. Analysis of phenylethanoid glycosides in the extract of herba Cistanchis by LC/ESI-MS/MS. Yao Xue Xue Bao 2000; 35:839-42. [PMID: 11218862].

15. Zhao Q, Yang X, Cai D, Ye L, Hou Y, Zhang L, Cheng J, Shen Y, Wang K, Bai Y. Echinacoside Protects Against MPP(+)-Induced Neuronal Apoptosis via ROS/ATF3/CHOP Pathway Regulation. Neurosci Bull 2016; 32:349-62. [PMID: 27432061].

16. Deng M, Zhao JY, Ju XD, Tu PF, Jiang Y, Li ZB. Protective effect of tubuloside B on TNFalpha-induced apoptosis in neuronal cells. Acta Pharmacol Sin 2004; 25:1276-84. [PMID: 15456528].

17. Wang Y, Li X, Wang J, Shi H, Bi W, Hou W, Zhang X. 7β-estradiol mediates upregulation of stromal cell-derived factor-1 in the retina through activation of estrogen receptor in an ischemia-reperfusion injury model. Graefes Arch Clin Exp Ophthalmol 2015; 253:17-23. [PMID: 24824367].

18. Zhang Z, Qin X, Tong N, Zhao X, Gong Y, Shi Y, Wu X. Valproic acid-mediated neuroprotection in retinal ischemia injury via histone deacetylase inhibition and transcriptional activation. Exp Eye Res 2012; 94:98-108. [PMID: 22143029].

19. Hughes WF. Quantitation of ischemic damage in the rat retina. Exp Eye Res 1991; 53:573-82. [PMID: 1743256].

20. Zhang Z, Tong N, Gong Y, Qiu Q, Yin L, Lv X, Wu X. Valproate protects the retina from endoplasmic reticulum stress-induced apoptosis after ischemia-reperfusion injury. Neurosci Lett 2011; 504:88-92. [PMID: 21939735].

21. Peinado-Ramón P, Salvador M, Villegas-Pérez MP, Vidal-Sanz M. Effects of axotomy and intraocular administration of NT-4, NT-3, and braini derived neurotrophicfactor on the survival of adult rat retinal ganglion cells. A quantitative in vivo study. Invest Ophthalmol Vis Sci 1996; 37:489-500. [PMID: 8595949].

22. Fang JH, Wang XH, Xu ZR, Jiang FG. Neuroprotective effects of bis(7)-tacrine against glutamate-induced retinal ganglion cells damage. BMC Neurosci 2010; 11:31-[PMID: 20199668].

23. Morrison JC, Nylander KB, Lauer AK, Cepurna WO, Johnson EC. Glaucoma drops control intraocular pressure and protect optic nerve in a rat model of glaucoma. Invest Ophthalmol Vis Sci 1998; 39:526-31. [PMID: 9501862].

24. Danias J, Shen F, Goldblum D, Chen B, Ramos-Esteban J, Podos SM, Mittag T. Cytoarchitecture of the retinal ganglion cells in the rat. Invest Ophthalmol Vis Sci 2002; 43:587-94. [PMID: 11867571].

25. Draper HH, Hadley M. Malondialdehyde determination as index of lipid peroxidation. Methods Enzymol 1990; 186:421-31. [PMID: 2233309].

26. Sun Y, Oberley LW, Li Y. A simple method for clinical assay of superoxide dismutase. Clin Chem 1988; 34:497-500. [PMID: 3349599].

27. Paglia DE, Valentine WN. Studies on the quantitative and qualitative characterization of erythrocyte glutathione peroxidase. J Lab Clin Med 1967; 70:158-69. [PMID: 6066618].

28. Cohen G, Dembiec D, Marcus J. Measurement of catalase activity in tissue extracts. Anal Biochem 1970; 34:30-8. [PMID: 5440916].

29. Lowry OH, Rosebrough NJ, Farr AL, Randall RJ. Protein measurement with the Folin phenol reagent. J Biol Chem 1951; 193:265-75. [PMID: 14907713].

30. Pietrucha-Dutczak M, Smedowski A, Liu X, Matuszek I, Varjosalo M, Lewin-Kowalik J. Candidate protein from predegenerated nerve exert time-specific protein of retinal ganglion cells in glaucoma. Sci Rep 2017; 7:14540-[PMID: 29109409].

31. Renner M, Stute G, Alzureiqi M, Reinhard J, Wiemann S, Schmid H, Faissner A, Dick HB, Joachim SC. Optic nerve degeneration after retinal ischemia/reperfusion in a rodent model. Front Cell Neurosci 2017; 22:11-254. [PMID: 28878627].

32. Smedowski A, Pietrucha-Dutczak M, Kaarniranta K, Lewin-Kowalik J. A rat experimental model of glaucoma incorporating rapid-onset elevation of intraocular pressure. Sci Rep 2014; 4:5910-[PMID: 25081302].

33. Pellegrini-Giampietro DE, Cherici G, Alesiani M, Carla V, Moroni F. Excitatory amino acid release and free radical formation may cooperate in the genesis of ischemia-induced neuronal damage. J Neurosci 1990; 10:1035-41. [PMID: 1969465].

34. Smedowski A, Liu X, Podracka L, Akhtar S, Trzeciecka A, Pietrucha-Dutczak M, Lewin-Kowalik J, Urtti A, Ruponen M, Kaarniranta K, Varjosalo M, Amadio M. Increased intraocular pressure alters the cellular distribution of HuR protein in retinal ganglion cells-A possible sign of endogenous neuroprotection failure. Biochim Biophys Acta Mol Basis Dis 2018; 1864:296-306. [PMID: 29107807].

35. Chida M, Suzuki K, Nakanishi-Ueda T, Ueda T, Yasuhara H, Koide R, Armstrong D. In vitro testing of antioxidants and

biochemical end-points in bovine retinal tissue. Ophthalmic Res 1999; 31:407-15. [PMID: 10474069].

36. Chen B, Caballero S, Seo S, Grant MB, Lewin AS. Delivery of antioxidant enzyme genes to protect against ischemia/reperfusion-induced injury to retinal microvasculature. Invest Ophthalmol Vis Sci 2009; 50:5587-95. [PMID: 19628743].

37. Lewden O, Garcher C, Morales C, Javouhey A, Rochette L, Bron AM. Changes of catalase activity after ischemia-reperfusion in rat retina. Ophthalmic Res 1996; 28:331-5. [PMID: 9032790].

38. Li Z, Lin H, Gu L, Gao J, Tzeng CM. Herba Cistanche (Rou Cong-Rong): One of the Best Pharmaceutical Gifts of Traditional Chinese Medicine. Front Pharmacol 2016; 7:41-[PMID: 26973528].

39. Lu CW, Lin TY, Huang SK, Wang SJ. Echinacoside Inhibits Glutamate Release by Suppressing Voltage-Dependent Ca(2+) Entry and Protein Kinase C in Rat Cerebrocortical Nerve Terminals. Int J Mol Sci 2016; 17:1006-[PMID: 27347934].

40. Jia Y, Guan Q, Guo Y, Du C. Echinacoside stimulates cell proliferation and prevents cell apoptosis in intestinal epithelial MODE-K cells by up-regulation of transforming growth factor-beta1 expression. J Pharmacol Sci 2012; 118:99-108. [PMID: 22186624].

41. Zhang Y, Long H, Zhou F, Zhu W, Ruan J, Zhao Y, Lu Y. Echinacoside's nigrostriatal dopaminergic protection against 6-OHDA-Induced endoplasmic reticulum stress through reducing the accumulation of Seipin. J Cell Mol Med 2017; 21:3761-75. [PMID: 28767194].

42. Zhang Y, Long H, Zhou F, Zhu W, Ruan J, Zhao Y, Lu Y. Therapeutic Effect of Cistanoside A on Bone Metabolism of Ovariectomized Mice. Molecules 2017; 22:197-[PMID: 28125037].

43. Yu Q, Li X, Cao X. Cardioprotective Effects of Phenylethanoid Glycoside-rich Extract from Cistanche deserticola in Ischemia-Reperfusion-Induced Myocardial Infarction in Rats. Ann Vasc Surg 2016; 34:234-42. [PMID: 27129809].

44. Choi JG, Moon M, Jeong HU, Kim MC, Kim SY, Oh MS. Cistanches Herba enhances learning and memory by inducing nerve growth factor. Behav Brain Res 2011; 216:652-8. [PMID: 20849880].

Articles are provided courtesy of Emory University and the Zhongshan Ophthalmic Center, Sun Yat-sen University, P.R. China. The print version of this article was created on 25 November 2018. This reflects all typographical corrections and errata to the article through that date. Details of any changes may be found in the online version of the article.